

## Chapter 3

### Theory

In this chapter the theory behind the SRMT will be presented. The first section will be devoted to a discussion of the equivalent network model for patch antennas. The foundation of the SRMT is the fact that the network model consists of a resonant parallel-RLC circuit. The influence of the probe on the input impedance and the network model is discussed in section 3.2. Sections 3.3 and 3.4 describe the basic working of the SRMT, and the improvement to end up with the Optimum Bandwidth Single LC-Resonator Matching Technique (SRMT) is provided in section 3.5.

#### 3.1 Equivalent network model for patch antennas

The design of microstrip patch antennas consists mainly of two parts. Firstly, the patch antenna must be resonant. Figure 3.1 shows a probe-fed and a microstrip-fed patch, showing the main design parameters available to design a patch antenna. The resonant length ( $L$ ) of the radiating structure, i.e. the patch, will normally be slightly shorter than half a wavelength at the centre frequency. The length depends on a number of variables, some of which are the substrate chosen as well as the electrical thickness of the patch antenna, i.e. the substrate height. The definition of this length is explained in terms of field distribution underneath the patch in [36]. Another important parameter to keep in mind with patch antenna design is the impedance at the feed position. The feed position ( $d$ ) and

patch width ( $W$ ) are the main contributors to this parameter, although the resonant frequency and input impedance cannot be designed independently. The width, length and feed position all have some level of influence on one another.

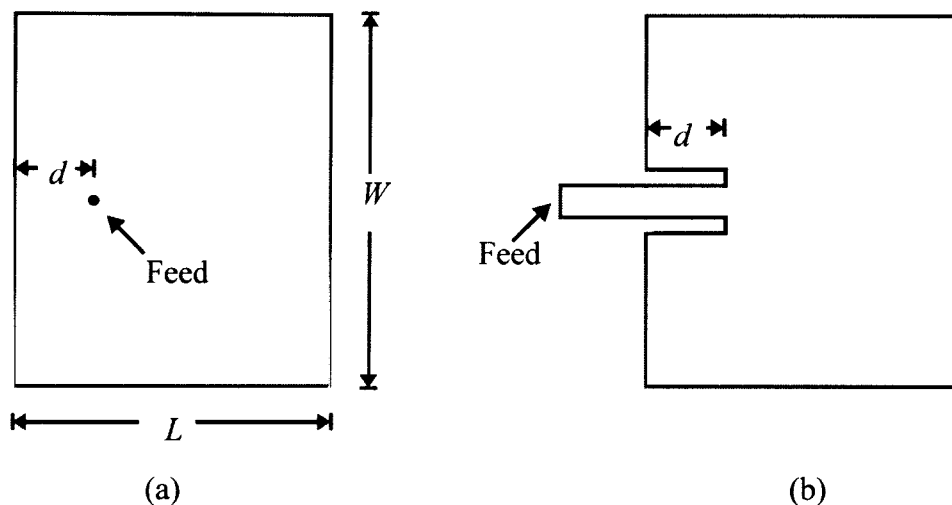


**Figure 3.1 Main design parameters for a rectangular microstrip patch antenna. (a) shows a probe-fed patch antenna, and (b) a microstrip-fed patch antenna**

The input impedance of a microstrip patch antenna has an RLC-circuit behaviour near its fundamental resonant frequency [1]. The feed mechanism (being either probe- or microstrip-fed) then further alters the impedance response. Mainly the probe-fed patch antenna will be considered in this dissertation. The probe adds a series inductance to the RLC-impedance. The simplified equivalent circuit of the input impedance of a probe-fed microstrip patch antenna, taken from [1], is shown in Figure 3.2.

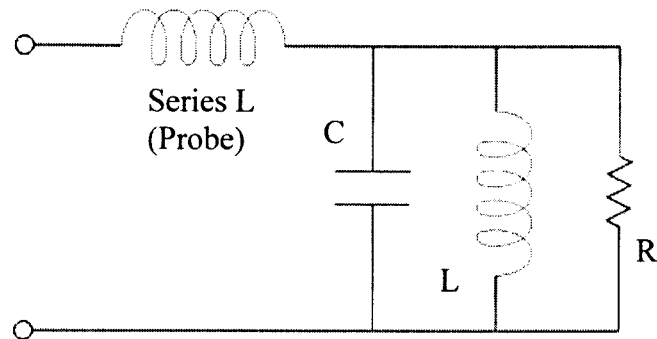


**Figure 3.2 Approximate equivalent circuit of the input impedance of a probed patch antenna**

The impedance frequency response of a parallel RLC-circuit is shown in Figure 3.3.

In illustration the following component values were used:  $R = 50 \Omega$ ,  $C = 17.5 \text{ pF}$  and  $L = 0.47 \text{ nH}$ .

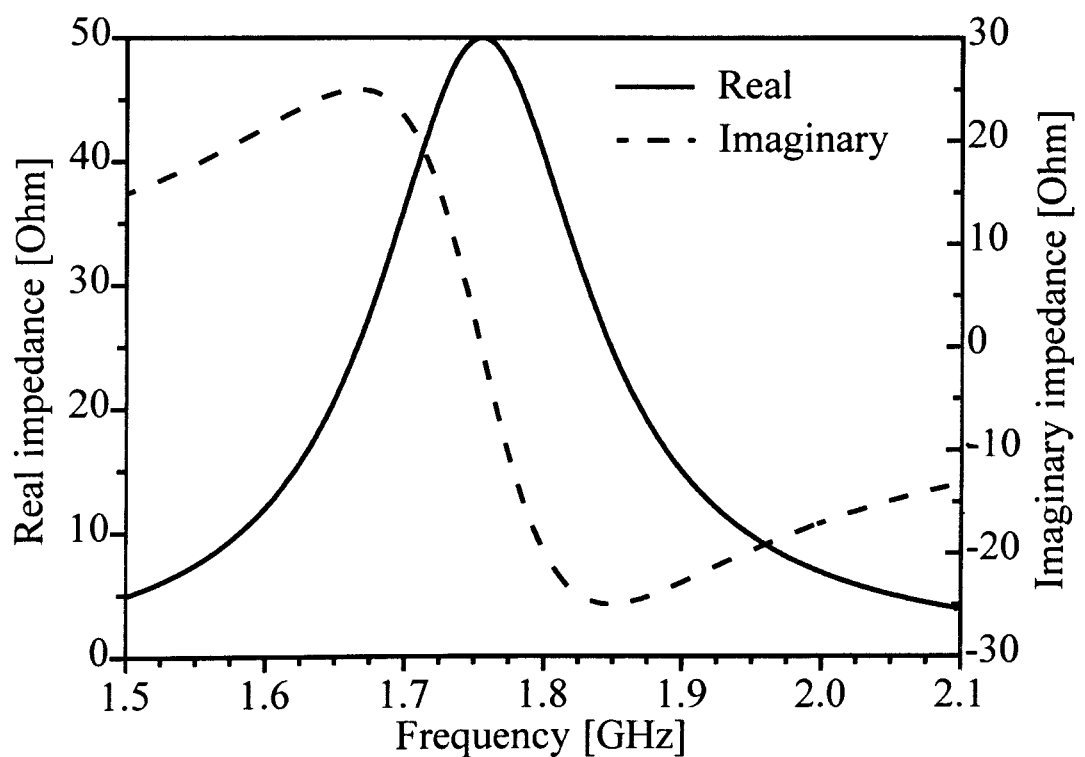


**Figure 3.3 Frequency response of a parallel RLC-circuit with a resonant frequency close to 1.8 GHz**

In Figure 3.3 the resonant frequency is clearly visible at 1.8 GHz as the imaginary impedance reaches zero. Incidentally the real impedance is also a maximum value at the resonant frequency for a pure parallel RLC-circuit. The real part of the impedance is symmetric around the resonant frequency, and the peak value of  $50 \Omega$  is the same as the resistor used in the example circuit. The imaginary part of the impedance shows odd symmetry around the resonant frequency. It is equal in size, but opposite in sign around this frequency. The RLC-circuit's impedance is thus equal in magnitude around its resonant frequency, but the impedance is inductive below and capacitive above the centre frequency. This type of frequency response is shown graphically on a Smith chart in Figure 3.4.

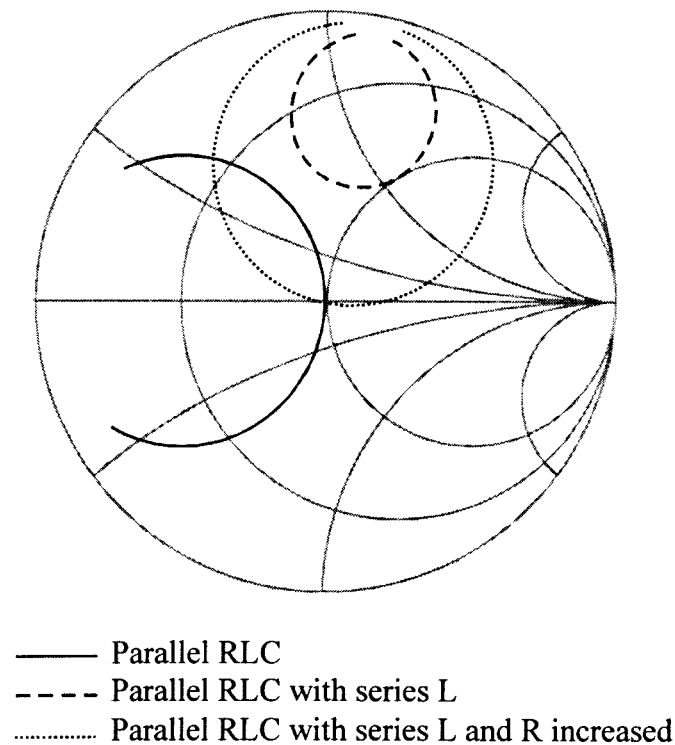


**Figure 3.4 Smith chart representation of impedance versus frequency behaviour for the various circuits discussed in this section**

The probe feed, commonly used for patch antennas, can be modelled as an additional series inductance to the patch input impedance. For the RLC-circuit discussed in the previous paragraph, a series inductor value of  $5.2 \text{ nH}$  is chosen to represent a probe-feed. The value is also for illustration only. In order to explain what is seen in Figures 3.4, 3.5 and 3.6 the

circuit shown in Figure 3.2 is mathematically derived. The final derived expression for the parallel-RLC circuit with a series inductor is given in (2). It is assumed that the reader has a basic knowledge of reactive impedance expressions as well as parallel and series component theory. Therefore the steps in between the derivation are omitted and only the initial and the final expression are presented.

$$\begin{aligned}
 Z_{in} &= Z_{L,serie} + Z_{RLC} \\
 &= Z_{L,serie} + \frac{1}{\frac{1}{R} + \frac{1}{Z_L} + \frac{1}{Z_C}} \\
 &= j\omega L_{serie} + \frac{j\omega RL}{j\omega C(j\omega RL) + j\omega L + R} \\
 &= \frac{\omega^2 RL^2}{(R - \omega^2 RLC)^2 + \omega^2 L^2} + j\omega L_{serie} + j \frac{\omega RL(R - \omega^2 RLC)}{(R - \omega^2 RLC)^2 + \omega^2 L^2} \quad (3)
 \end{aligned}$$

The series inductance is added to the impedance of the parallel-RLC circuit. In equation (3) the final expression illustrates how the term obtained with the series inductance is imaginary, and the term can be considered part of the imaginary impedance only. The real impedance has no reference to the component ( $L_{serie}$ ) and is therefore unaffected by the addition of the series inductance. In the region of 1.8 GHz an inductor of 5.2 nH results in a series imaginary impedance of 58.8  $\Omega$  being added to the imaginary impedance. Figure 3.5 graphically illustrates how the imaginary curve is literally lifted. The amount that the curve is lifted varies (i.e. the impedance added from  $L_{serie}$ ), because the inductor impedance is frequency sensitive. On the Smith chart in Figure 3.4 the dashed line graphically illustrates the real and imaginary curves obtained from (3) with the series inductor included. Interesting to note is the major reduction encountered in the size of the locus on the Smith chart, from the solid curve representing the original parallel RLC-circuit, to the identical parallel RLC-circuit with the series inductor added. There is no region where the locus gets close to the real axis. In Figure 3.5 the imaginary curve is also very high above the  $j0 \Omega$  value over the whole frequency range considered.

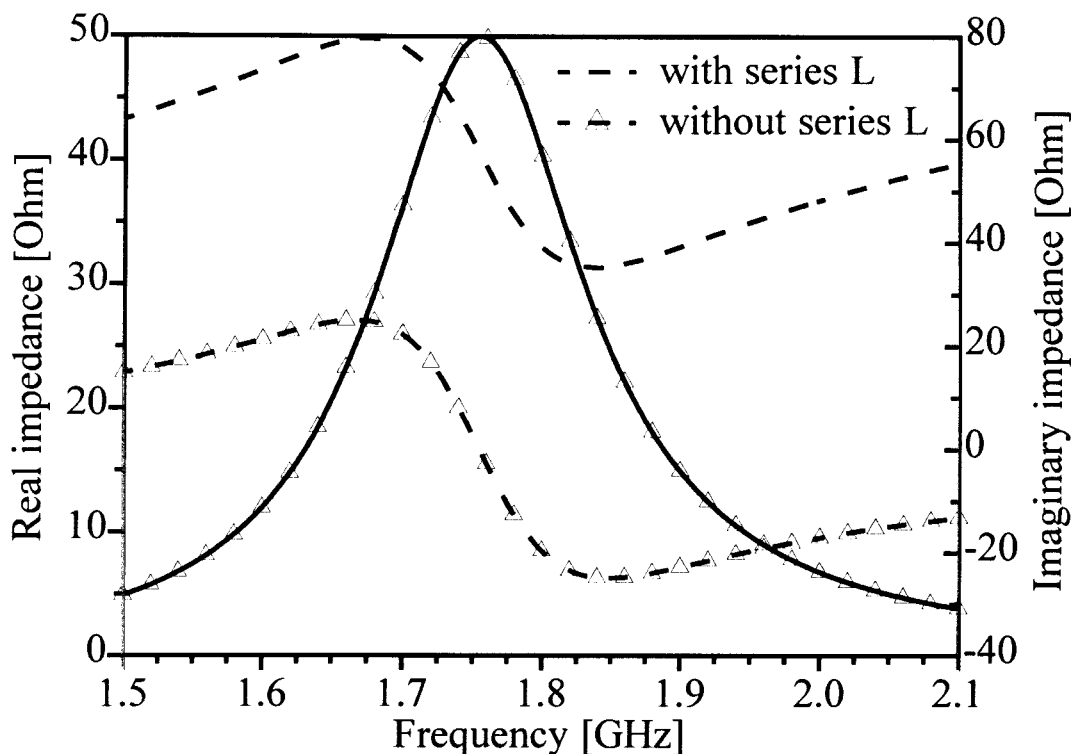


**Figure 3.5 Comparison of the impedance of a parallel RLC-circuit with and without the addition of a series inductor**

Electrically thicker patch antennas often have real impedance peaks that are higher than the required value. The frequency point where the antenna is matched to  $50\ \Omega$  is then not at the peak of the real impedance curve, but on the slope. The series inductor with the parallel-RLC model discussed so far in this section is part of a building block to try to understand this impedance behaviour of electrically thick patches. Equation (3) shows that the imaginary term of the input impedance includes all the elements ( $R$ ,  $L$ ,  $C$  and  $L_{series}$ ) used in the model. Varying either  $L$  or  $C$  will ultimately alter the resonance of the parallel RLC-circuit and changing  $L_{series}$  will only result in the imaginary curve lowering or lifting. Variation in  $R$  proved to be a viable option. The value of  $R$  was increased to  $120\ \Omega$ , and the dotted locus shown in Figure 3.4 illustrates the effect of doing this. The curve passes through the  $50\ \Omega$  point. More important to note is the graph presented in Figure 3.6. The imaginary curve has changed dramatically. The offset of the imaginary curve is still  $58.8\ \Omega$  as originally obtained from  $L_{series}$ , but the curve has much lower and upper limit values and

reaches  $j0 \Omega$  in the frequency range considered. In conjunction with the imaginary curve that has changed, the real impedance has inevitably also changed with the increased R.

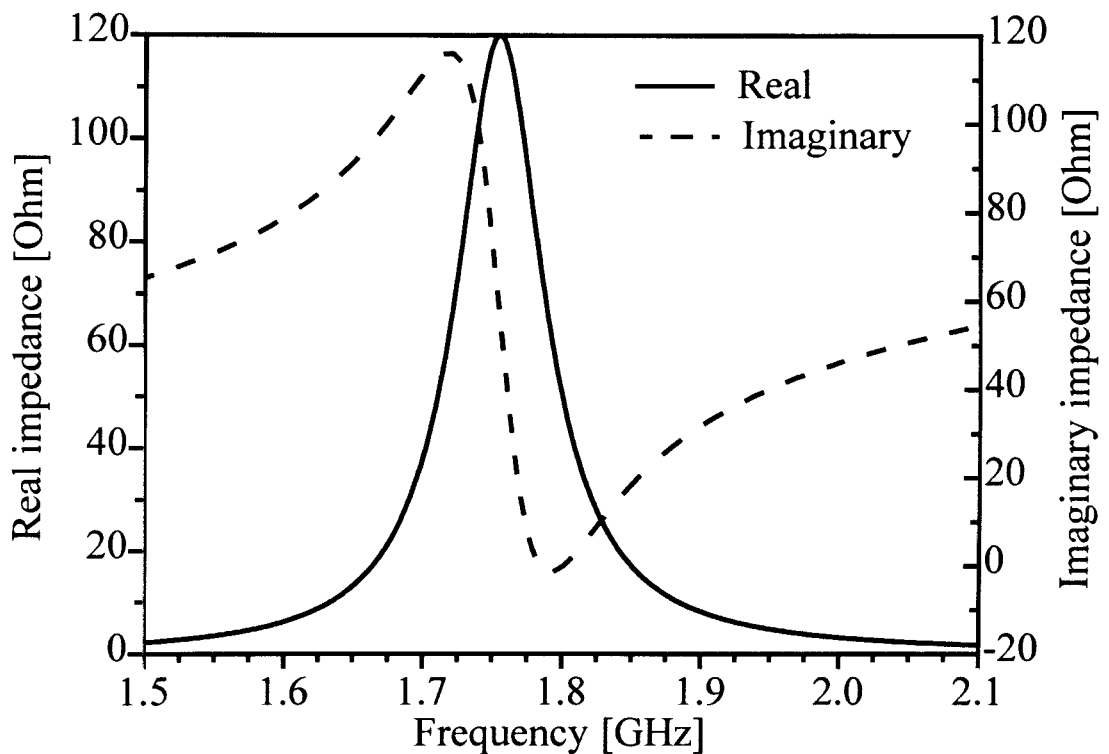


**Figure 3.6 Impedance response versus frequency with the addition of a series inductor and increased real impedance**

The impedance of the RLC-circuit that the section started was symmetric around the resonant frequency. Resonant frequency is defined as the frequency where the imaginary part of the impedance reaches zero and the total input impedance is purely real. Figure 3.6 and the coinciding Smith chart locus in Figure 3.4 show how a series inductance disturbs this symmetry, and an increased R in effect restores a level of resonance, but with no symmetry around the centre frequency anymore. This type of input impedance, with no real noticeable symmetry, is a very common sight in microstrip patch antenna design. In the next section it will be shown how symmetry can actually still be obtained, and that it can then be used to one's advantage.

### 3.2 Retrieval of symmetry in the impedance curves around the minimum reflection frequency point

Section 3.1 started with a simple parallel RLC-circuit, and ended with a more complicated circuit, shown in Figure 3.2. It was shown how one can initially have an ideal impedance curve (Figure 3.3 and 3.4) and how this curve is almost never the graph one ends up to work with (Figure 3.6). In this section it will be shown how the effect of the series inductor and increased R of the input impedance can be reversed in terms of frequency impedance behaviour. This will be done with actual simulated patch antenna data.

The patch used as design example for the matching circuit principle is shown in Figure 3.7.

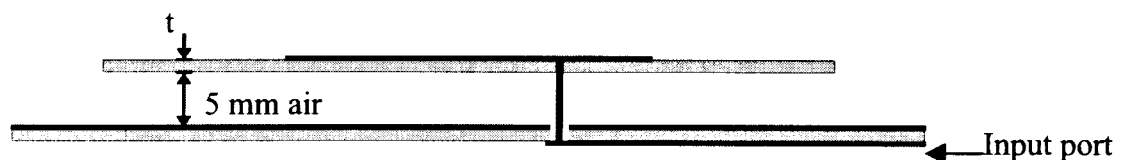


**Figure 3.7 Probe-fed patch antenna example. The input impedance is measured and referenced at the ground plane interface**

The patch antenna presented in Figure 3.7 is etched on dielectric substrate with dielectric constant  $\epsilon_r = 3.05$ , loss tangent  $\tan\delta = 0.003$  and thickness  $t = 1.524$  mm. The material is GML-1000 and supplied by GIL Technologies [38]. The feed line and matching network considered later are etched on dielectric substrate with  $\epsilon_r = 3.53$ ,  $\tan\delta = 0.017$  and  $t = 1.575$  mm. Material is MC3D, also by GIL Technologies [39]. Figure 3.8 presents the real and imaginary impedance curves of the patch antenna of Figure 3.7 near its designed resonant frequency, chosen to be 1.8 GHz. The graphical response is shown on a Smith chart in Figure 3.9. The solid black line on the Smith chart is the response coinciding with the curves presented in Figure 3.8. Take note of the close correlation between the curves shown in Figures 3.8 and 3.6.



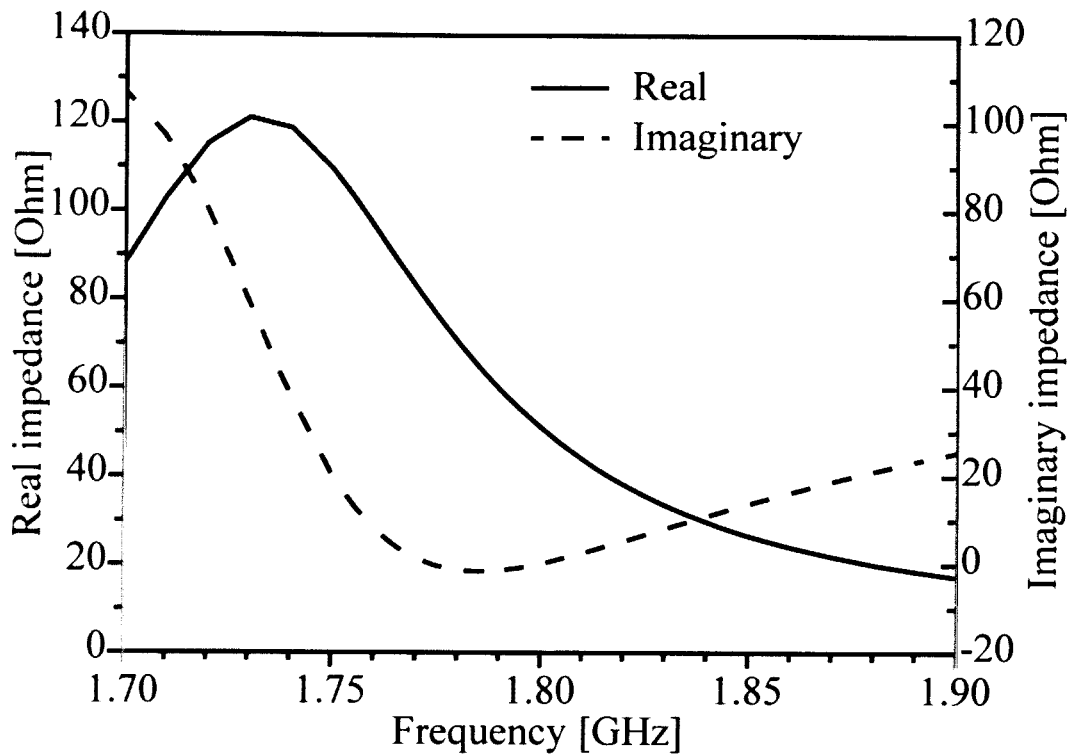


**Figure 3.8** Simulated input impedance of the probe-fed microstrip patch antenna shown in Figure 3.7

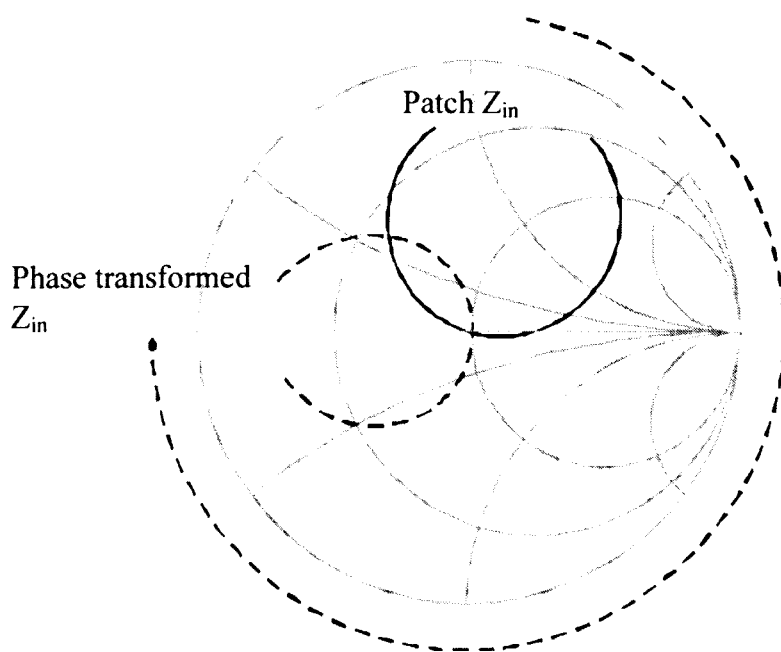


**Figure 3.9** Input impedance of the example patch antenna as plotted on the Smith chart

In the previous section emphasis was placed on the fact that no symmetry is available in the impedance response. The series inductance associated with the probe-feed acts as a transmission line with some level of impedance transforming. This becomes evident as the Smith chart is considered as graphical aid. The phase and impedance transforming effect of the inductor can be seen in Figure 3.4. Additional phase transforming will result in an impedance response that is again similar to a response expected from a relatively simple parallel RLC-circuit. Figure 3.10 shows the analogy of phase transforming the impedance.

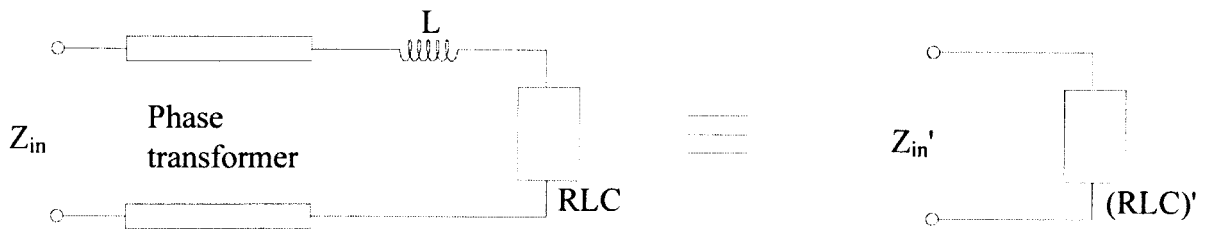


**Figure 3.10 Effective result of phase transformation applied to patch antenna input impedance**

The phase transformed data for the patch antenna is included on the Smith chart in Figure 3.9. The locus changes somewhat in shape. This is due to the fact that the phase transformation is a function of frequency, and only the centre frequency has the exact numerical transformation expected.

The real and imaginary impedance curves of the newly obtained input impedance are shown in Figure 3.11. A peak real impedance value is obtained at the resonant frequency and the imaginary impedance curves resemble odd symmetry around the resonant frequency, i.e. opposite in sign but equal in magnitude.

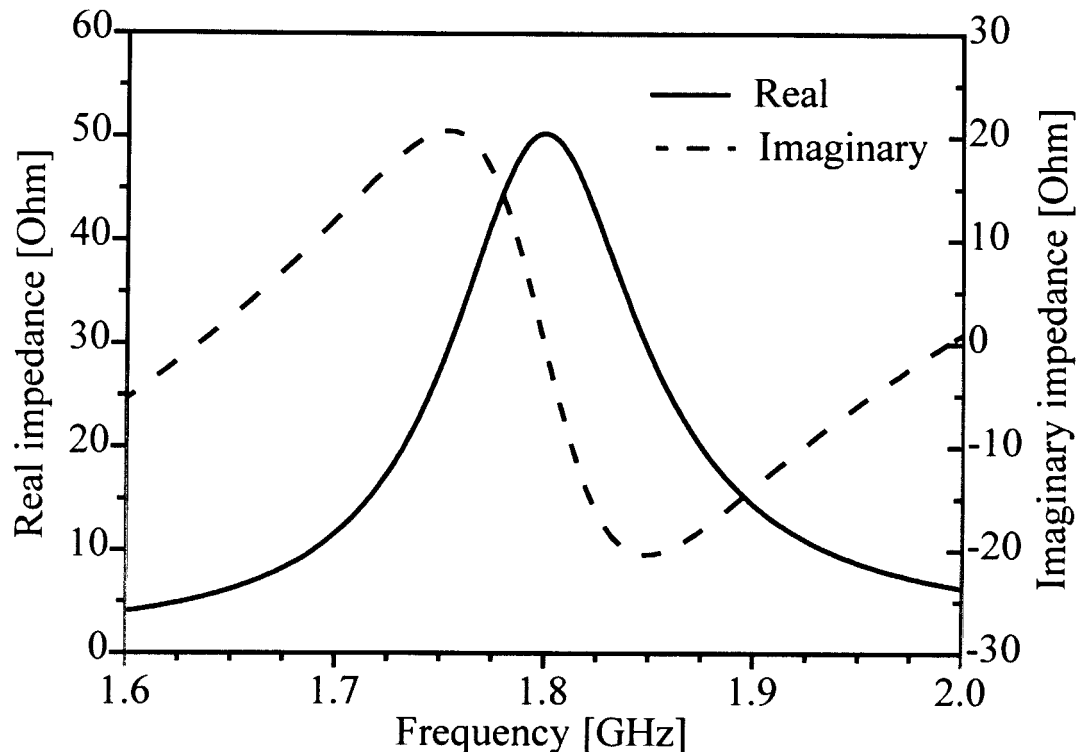


**Figure 3.11 Impedance curves of the phase transformed patch antenna input impedance**

### 3.3 Reduction of imaginary impedance

The imaginary impedance of the phase transformed patch antenna is inductive at frequencies lower than the resonant frequency and capacitive at frequencies higher than the centre frequency. If one considers a parallel LC-combination without the resistor and series inductance in the circuit diagram as presented in Figure 3.2, this is precisely what would happen with this combination at and around its resonant frequency. The matching technique presented in this dissertation aims to obtain a bandwidth improvement by effectively cancelling the imaginary component of the input impedance at frequencies close to the resonant frequency.

A parallel LC-combination is inductive at low frequencies and capacitive at high frequencies, where low and high are defined relative to the resonant frequency. This means that a parallel combination of the LC-circuit and a load that is inverse, i.e. capacitive at low frequencies and inductive at high frequencies, will result in a cancellation of the total reactive component. A patch antenna impedance locus as presented in Figure 3.11 is phase transformed to obtain an RLC-equivalent response. When the phase transformation is not taken as far as in Figure 3.9, but rather a line length at centre frequency of  $90^\circ$  shorter, the curve shown in Figure 3.12 is obtained.

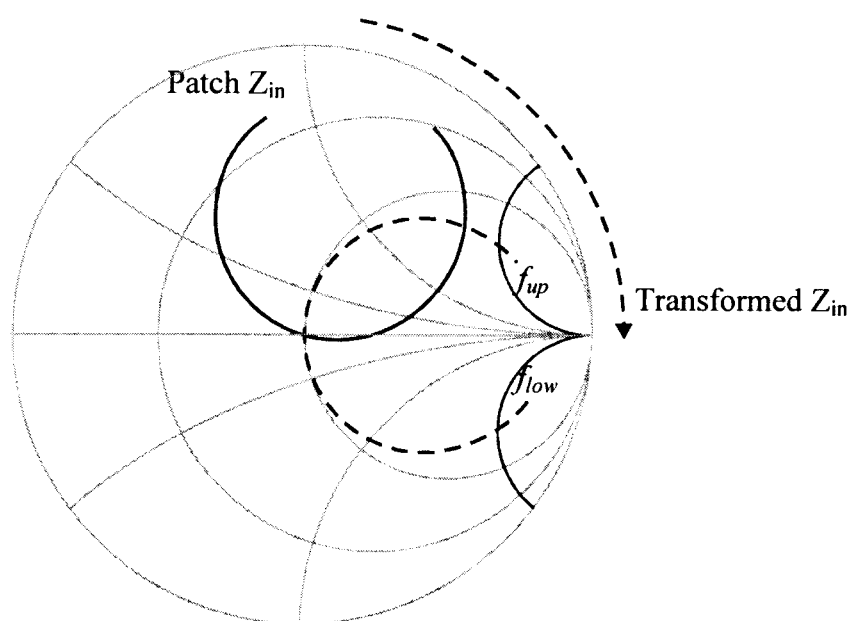


**Figure 3.12 Phase transformation of patch antenna to obtain a capacitive reactive component at low and inductive component at high frequencies**

It is mentioned in the previous paragraph that one would like to work with a parallel combination between the proposed LC-circuit and the load impedance. Therefore it might prove more useful to work with admittance instead of impedance values. When placing components in parallel the total admittance will be a simple summation of each component's individual admittance value, as is shown in equation (4).

$$Y_L + Y_C + Y_{Load} = Y_{Total} \quad (4)$$

The admittance curves obtained with the phase transformation illustrated in Figure 3.12 are shown in Figure 3.13. The shape is similar to the ideal parallel RLC-circuit. In other words, a peak real admittance value is obtained at the centre frequency, and the imaginary admittance is equal in magnitude but opposite in sign around the centre frequency. Also, a positive imaginary value now implies a capacitive component while a negative reactive value represents an inductive component.

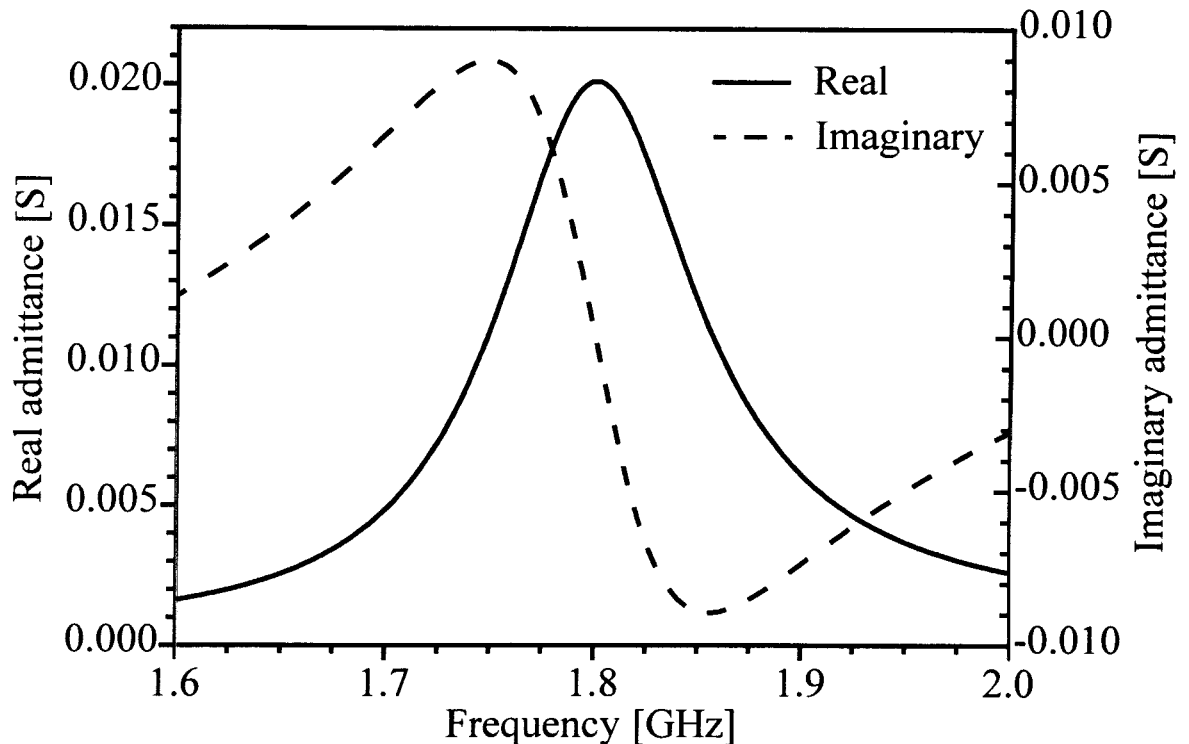


**Figure 3.13 Admittance curves associated with the phase transformation done in Figure 3.12**

An LC-circuit has a straight-line admittance frequency response crossing the zero admittance value at its resonant frequency. The solid line in Figure 3.14 represents the admittance of a parallel LC-section with a resonant frequency of 1.8 GHz. When a LC-circuit is used to cancel out overall reactive components, care must be taken that resonance for both the load and the added LC circuit occurs at the same frequency. This will result in the LC-circuit added in parallel having no effect on the admittance at the centre frequency, while cancelling the antenna imaginary admittance values at other frequencies. This is mathematically presented in equation (5).

$$\text{Im}[Y_{f_c}] = \text{Im}[Y_{f_c}] = 0 \quad (5)$$

The subscript *-f<sub>c</sub>-* denotes centre frequency, and the subscripts *-LC-* and *-Load-* denote the LC section and load admittance respectively.

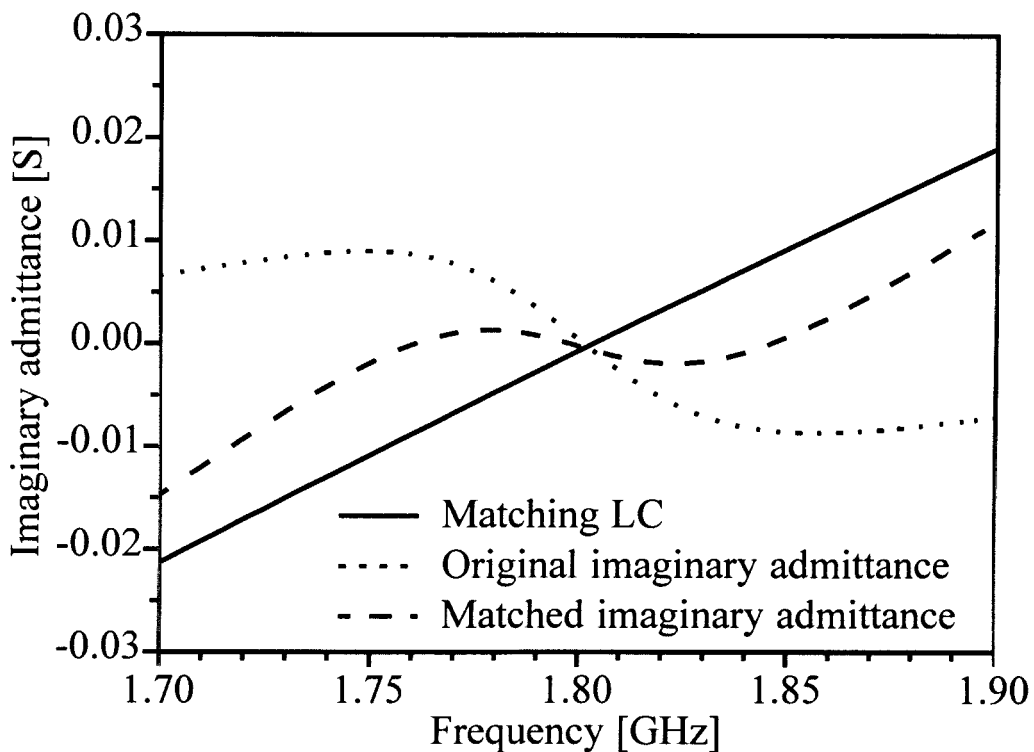


**Figure 3.14 Effective cancellation of the imaginary part of the load admittance with the addition of a parallel LC-section**

The addition of a parallel LC-section means that only the imaginary component of the admittance will change and the real part will remain the same. This is shown in equations (6) and (7).

$$\text{Im}[Y_{Total}] = Y_L + Y_C + \text{Im}[Y_{Load}] \quad (6)$$

$$\text{Re}[Y_{Total}] = \text{Re}[Y_{Load}] \quad (7)$$

Figure 3.15 includes the real admittance obtained in Figure 3.14 and shows what happens to the parameter before and after the LC-section is added to the phase transformed load.

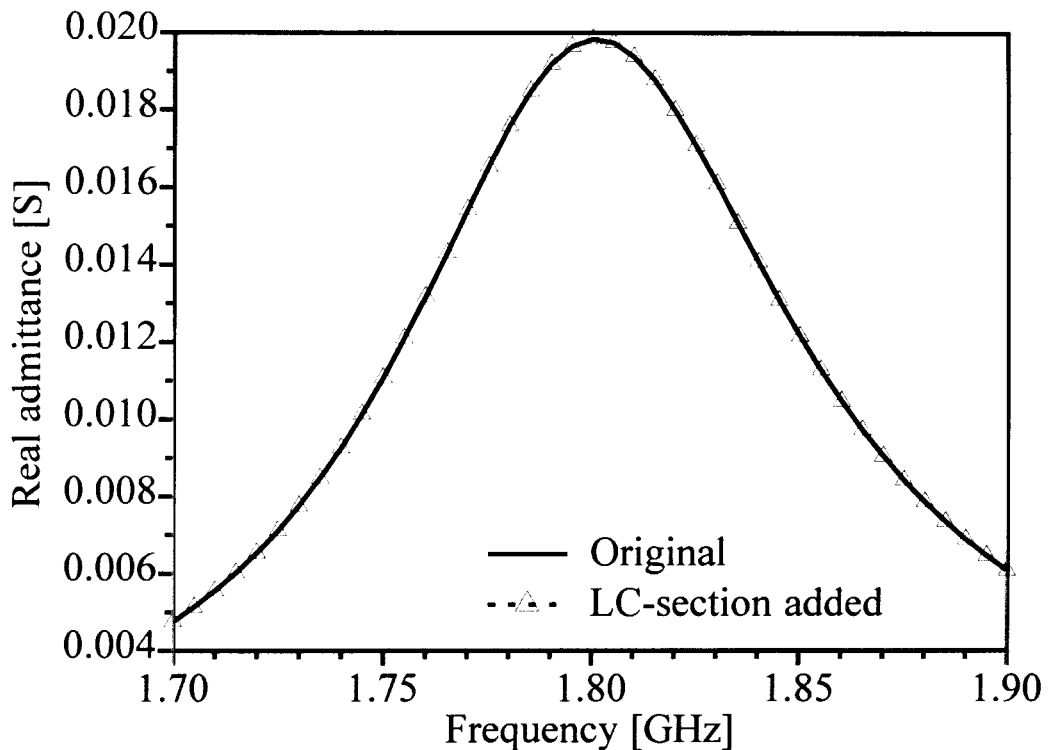


**Figure 3.15 Effect on the real admittance with the addition of a parallel LC-section to the load admittance**

In the last two figures it can be seen clearly how the admittance of a phase transformed patch antenna was changed in such a way that the imaginary admittance varies less around the centre frequency, while the real admittance remains virtually unchanged. The Smith chart representation illustrating the effect of this addition of the LC-section is shown in Figure 3.16. An eye-shaped locus is created on the Smith chart. This eye is the result of the unchanged real admittance, while the reactive component is now more constant around the centre frequency than before.

The Smith chart representation in Figure 3.16 illustrates how the eye-shaped locus makes a loop that remains within a certain VSWR circle on the Smith chart. The reflection coefficient simulated for this circuit, before and after the addition of the LC-section, is presented in Figure 3.17.

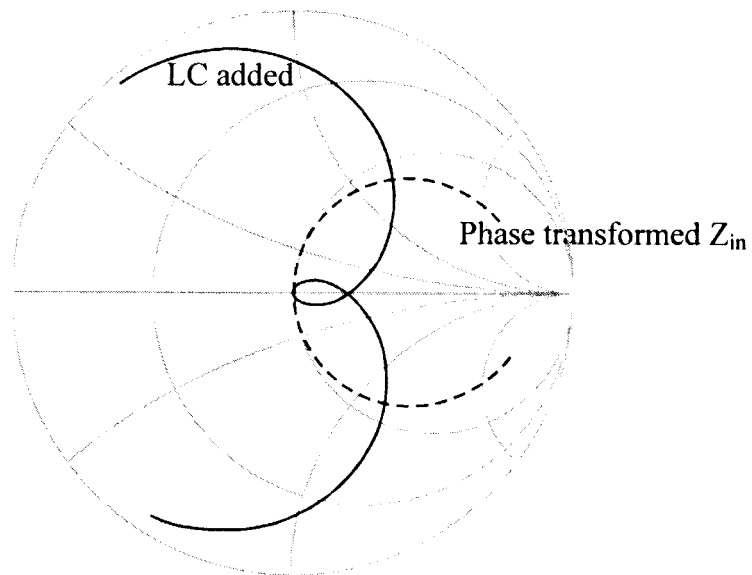


**Figure 3.16 Addition of a parallel LC-section to the phase transformed load impedance**

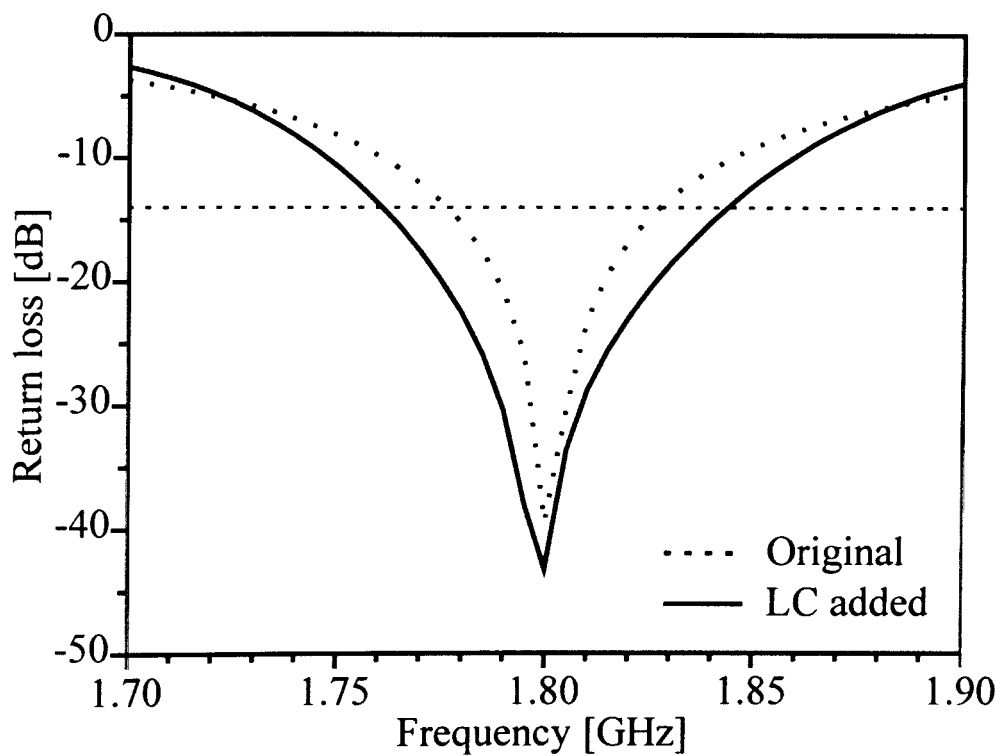


**Figure 3.17 Effective improvement of the return loss with the addition of an LC-section to the phase-transformed load**



In Figure 3.17 it is clear that there is a bandwidth improvement. More precise design procedures will be discussed in the following section, including additional improvement as well as design criteria.

### 3.4 Design of the LC-network for bandwidth improvement

In the previous section the fact that an added parallel resonant circuit can result in a patch antenna having an improved impedance bandwidth was illustrated. This is the underlying principle on which the coupled lines matching circuit discussed in [17, 18] is also based. The mathematical approximation of the coupled lines is a resonant circuit similar to a parallel LC-circuit with a transformer [21]. This additional resonator is then effectively responsible for the improvement in impedance bandwidth of the patch antenna and array. In [17, 18] not much detail of the working of the feed circuit is presented.

The first step in the design of a matching LC-section is to find the length of the phase transforming transmission line that will lead to symmetry in the real admittance, and odd symmetry in the imaginary admittance around the centre frequency. For this basic condition two possibilities are valid and must therefore be defined in more precise detail. The real admittance should have a maximum value at the centre frequency and the imaginary admittance should be positive below and negative above the resonant frequency. This definition is presented graphically in Figures 3.12, 3.13 and 3.16. This is a part of the design process where the graphical aid of the Smith chart is of great advantage, and it is suggested that this method (the graphical method) be used to find the correct line length.

The guidelines for the phase transformation mentioned in the previous paragraph should be used in conjunction with the graphical aid of the Smith chart. The statement of the maximum real admittance shows one the exact point where the locus on the Smith chart tends to turn away from the centre again, provided that one is relatively close to the correct phase position. In conjunction with the real admittance, the imaginary admittance should exhibit close to identical values but opposite in sign around the resonant frequency. The unmatched curve in Figure 3.16 illustrates this scenario, where the maximum real

admittance will be at the left-hand side of the locus, also being the centre frequency of the curve. Similarly, the curve is identical above and below the real axis.

The next step is to find the parallel LC-combination that will result in the most effective reduction in the reactive components around the centre frequency leading to an improved impedance bandwidth. Figure 3.14 illustrates what happens to the final imaginary admittance when the resonant admittance is added to the system. In the area close to the resonant frequency the imaginary admittance has a negative slope. The LC-circuit on the other hand has a positive slope. Summation of these two functions results in a reduction in the slope of the imaginary component. There are now three frequency points where the reactive components are zero. The centre point is the resonant frequency, where both the phase-transformed antenna admittance and the LC-circuit should have a zero reactive component. The other two frequency points are in the ideal case spaced equally far from the centre value at a lower and higher frequency. These two points, in conjunction with the resonant frequency, are the main design parameters for the LC-circuit. A simple set of equations can be implemented to calculate what the required capacitor and inductor values should be. The equations are shown in (8) and (9) and should be used in conjunction with (10) and (11).

$$Y_{low} = Y_{C_{low}} + Y_{L_{low}} \quad (8)$$

$$Y_{up} = Y_{C_{up}} + Y_{L_{up}} \quad (9)$$

The admittance of the capacitor and inductor are defined as follows:

$$\begin{aligned} Y_C &= j\omega C \\ \therefore Y_C &= j2\pi fC \end{aligned} \quad (10)$$

$$\begin{aligned} Y_L &= \frac{-j}{\omega L} \\ \therefore Y_L &= \frac{-j}{2\pi fL} \end{aligned} \quad (11)$$

The symbol  $Y$  denotes the admittance, with the subscript  $-C-$  and  $-L-$  indicating whether it is for the capacitor or inductor respectively. The further defined subscripts  $-low-$  and  $-up-$  show the frequency, in other words for the lower or upper frequency edge of the matching circuit. In equations (10) and (11) the  $-low-$  and  $-up-$  subscripts are omitted. To find the required admittance ( $Y$ ) one must substitute the specific frequency ( $f$ ) that is needed, being either the lower or upper frequency. From these equations one ends up with two unknowns,  $L$  and  $C$ , and two basic equations, (8) and (9). Solving them simultaneously results in the required solution. Equation (12) now gives the resonant frequency of the LC- circuit.

$$f_c = \frac{1}{2\pi\sqrt{LC}} \quad (12)$$

Earlier in this section it was mentioned that the LC-circuit and the antenna should have resonant frequencies,  $f_c$ , that are ideally exactly the same. Despite this important fact, it is not part of the actual design process. The reason is that when the phase shift as shown in Figure 3.12 is done accurately, the resonant frequency ( $f_c$ ) will automatically be correct. If one uses a slightly incorrect phase shift the resonant frequency will not be precise. This will lead to a marginal capacitance or inductance when the LC-circuit is added where the system was assumed to be resonant, and a slight asymmetry in the final return loss can be seen. Fine-tuning of the component values once the matching network is combined with the patch antenna will solve this.

In equations (8) and (9) two frequencies were defined, namely  $f_{low}$  and  $f_{up}$ . These are the frequencies where the parallel-resonant circuit must cancel the imaginary component of the phase transformed antenna admittance completely in such a way that total admittance becomes real. These frequency values are not chosen arbitrarily, but are chosen according to the real admittance curve. In Figure 3.15 it is evident that the addition of the LC-network to the circuit does not alter the real admittance. This property of the LC-circuit provides the solution for choosing the frequency points where the imaginary component should be zero. When the reactive component of the input admittance is effectively cancelled with the addition of the resonant section at the frequencies where the real admittance would just fall within the required VSWR specification when considered alone,

the best bandwidth improvement is obtained. Results for a test conducted on the patch example shown in Figure 3.7 to verify the validity of this statement is shown in Figure 3.18. The bandwidth was tested for a VSWR less than or equal to 1.5:1. Without the addition of an external circuit the antenna itself has a return loss better than  $-14$  dB between 1.773 and 1.825 GHz, a bandwidth of 2.89%. The phase-transformed admittance was considered and various LC-combinations were chosen to reduce the overall reactive component of the admittance. The capacitance and inductance values are chosen to cancel the imaginary admittance at a specific frequency (assuming symmetry in impedance, i.e. the lower and upper real admittance is roughly the same) is plotted against percentage bandwidth improvement in Figure 3.18. For a VSWR  $< 1.5:1$  the real admittance when considered alone should be either 0.0133 S or 0.03 S.

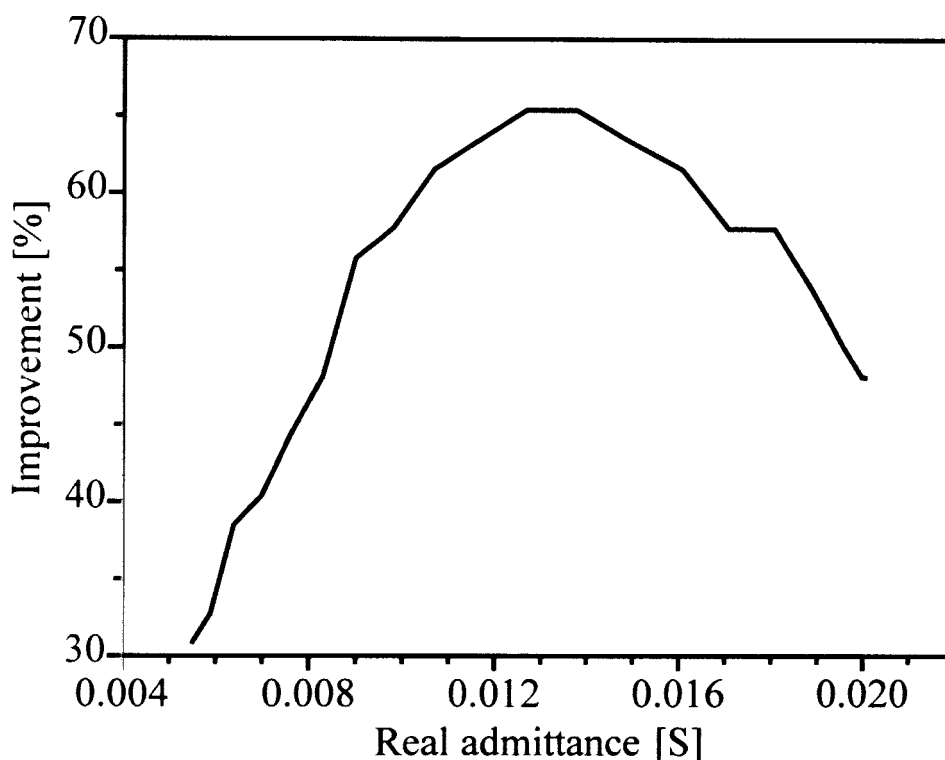


**Figure 3.18 Percentage improvement obtained for real admittance values where the LC-circuit is designed to cancel the imaginary component**

From Figure 3.18 it is clear that a bandwidth improvement in the order of 65% can be obtained when the LC-circuit is designed in such a way that it will result in real admittance values that fall just within specifications when considered alone. The lower edge for a  $V_{SWR} < 1.5$  is 0.0133 S. The actual percentage (i.e. 65%) is a value that is only valid for this patch antenna example, and it will vary for different types of antennas. The most important deduction that can be made from the graph in Figure 3.18 is that the maximum possible improvement will be obtained when the matching LC-section is chosen to cancel the imaginary admittance at the frequencies where the real admittance considered alone will fall just within the VSWR specification.

### 3.5 Transformation of the real admittance

In the previous section it was explained in detail how it is possible for the LC-section not only to improve the impedance bandwidth of a microstrip patch antenna, but also that an optimal solution can also be found for an LC-circuit. In Figures 3.16 and 3.17 the result is shown on both the Smith chart and the Cartesian plane. When the mentioned technique is suggested as an impedance enhancement method, a quick glance at these two graphs suggests some room for additional improvement. On the Smith chart a so-called eye is created when the LC-circuit is added. At the centre frequency the impedance locus passes through  $50 \Omega$ . A better bandwidth improvement factor is possible when the centre frequency does not pass through  $50 \Omega$ , but when the centre of the eye is located at  $50 \Omega$ . The displacement of the eye-shaped locus on the Smith chart to the centre of the chart will result in the graph of Figure 3.17 not having a near perfect match at the centre frequency, but rather a more steady and broader frequency band response below a certain reflection coefficient value. This section is devoted to explaining and illustrating how this is done, and what the effect on the effective bandwidth improvement of this extra step is.

The accomplishment of an optimally wide impedance bandwidth by creating a mismatch at the centre frequency is a relatively simple procedure. It is done by transforming the real part of the impedance (alternatively admittance) as part of the matching procedure. As a result of the symmetric nature of the matching technique discussed, a quarterwave matching section poses the simplest solution. A few factors that one needs to keep in mind are that the quarterwave transformer will transform the real admittance to another form, and that the quarterwave length in itself is only valid at the centre frequency. At any other frequency the line will either be electrically longer or shorter.

First the issue of line length is considered. The quarterwave match is known to be fairly wideband in its performance. Although the term wideband is commonly used, and generally understood, it must be defined more precisely. A wideband microstrip patch is most often a patch with a 20 to 30% impedance bandwidth. On the other hand, wideband antennas can reach bandwidths with a frequency ratio of up to 40:1. For the real wideband

antenna range, quarterwave matching will not provide an answer, but for patch antennas these transformers are wider than the antenna and will provide a good match.

The second consideration for quarterwave matching circuits is the phase transforming property of the transmission line. The  $90^\circ$  section of transmission line results in a real admittance with a minimum value at the centre frequency and higher values being reached at the edge of the frequency ranges considered. This is shown in Figure 3.19. This phase-transforming property of a quarterwave section must be kept in mind when designing a matching circuit. The next few paragraphs will illustrate how this is done.

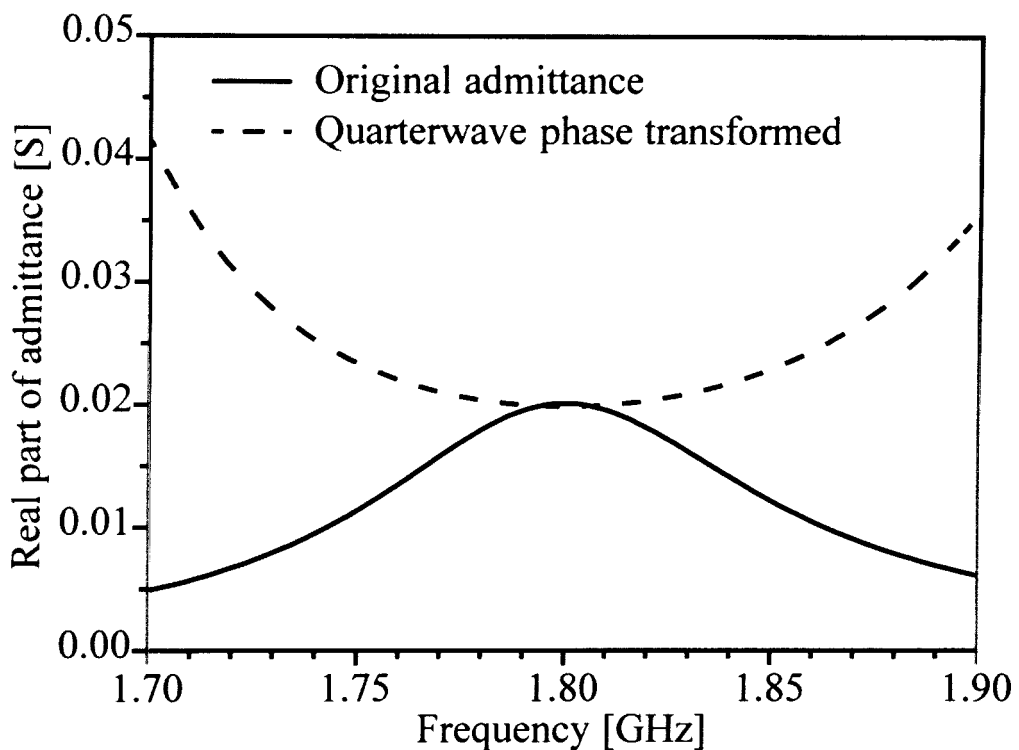


**Figure 3. 19 Phase transforming of the real admittance with a  $90^\circ$  line**

The inclusion of a quarterwave transmission line in the matching circuit leads to a slightly enlarged circuit. At first glance the possibility of including the impedance transformer in the first phase transforming line section seems to be the best option. The problem encountered is, however, that the line length for phase transformation will not reach a value of  $90^\circ$ . The only alternative position for the quarterwave impedance (admittance) transformer is after the LC-circuit.

The design of the transformer can be integrated as part of the matching circuit design process. The procedure will change slightly, since the real impedance must first be transformed before the LC-section can be calculated.

Considering the so-called eye on the Smith chart (Figure 3.16) it becomes clear that the front end of the locus (the left-hand side of the eye in Figure 3.16) can move left to the specified VSWR circle on the Smith chart. The effect of this left-sided movement in Figure 3.16 will possibly be an increase in VSWR bandwidth, but more importantly the original band considered (Figure 3.17) will remain below the predefined VSWR. In conjunction with the displacement of the locus on the Smith chart, an increase in diameter of the locus can also contribute to an improvement in bandwidth operation. This is possible when the LC-circuit is designed for a lower  $f_{low}$  and higher  $f_{up}$ .

The inclusion of the quarterwave transformer line results in a  $90^\circ$ -phase transformation. The curve will then be orientated in similar fashion to the locus included in Figure 3.9. The implication is that the real admittance curve has a minimum value at the centre frequency, instead of the maximum value that was intended originally (Figure 3.19). The LC-section is placed before the transformer, and the matching principle will remain the same. The only difference will be that the anticipated real admittance (after the transformer) will determine  $f_{low}$  and  $f_{up}$ .

Working with the edge of the VSWR circle on the Smith chart, the centre frequency real admittance must be transformed to the minimum allowable value, according to (13).

$$Z_{\lambda/4} = \frac{1}{\sqrt{Y_{Load} \cdot Y_{min}}} \quad (13)$$

Equation (13) is an alternative formulation of the standard quarterwave transformer expressed in terms of load admittance ( $Y_{Load}$ ) for the phase-transformed admittance and the required minimum admittance ( $Y_{min}$ ) used for improved bandwidth. For the test case considered previously the minimum value for a VSWR of 1.5:1 is 0.0133 S, and for a VSWR of 2:1 it is 0.01 S. Assuming that the original admittance is 0.02 S, this results in a transmission line impedance of 61.2  $\Omega$  or 70.7  $\Omega$  respectively.



The transformer line impedance calculated with (13) is initially used for the centre frequency transformed admittance. In addition, the transmission line also determines the newly obtained edge frequencies,  $f_{low}$  and  $f_{up}$ , where the imaginary component can be cancelled so that the real value that is left will fall within the VSWR specification. The impedance (admittance) transformer is normally designed to work mainly for real impedance values. In this matching technique the aim is to create two additional frequency points where the admittance will also be a real value. From Figure 3.19 it is clear that the edge value for the transformed admittance is at a maximum allowable value. For a VSWR of 1.5:1 this is 0.03 S and for a VSWR of 2:1 it is 0.04 S.  $Z_{\lambda/4}$  is a known parameter from (13), and it is also known that the admittance will be real at the maximum value due to resonance. In order to find the frequencies where the LC-circuit must cancel the imaginary admittance equation (14) is implemented (derived from (13)).

$$Y_{Load} = \frac{1}{Y_{max} \cdot Z_{\lambda/4}^2} \quad (14)$$

The phase-transformed (before admittance transformation) admittance of the patch antenna ( $Y_{Load}$ ) is now considered to be the unknown parameter. The impedance of the transformer ( $Z_{\lambda/4}$ ) and the maximum admittance ( $Y_{max}$ ) that falls within specification are used in (14) to determine what admittance in the original curve ( $Y_{load}$ ) will be transformed to the required load after the transformation. With a VSWR of 1.5:1 and  $Z_{\lambda/4} = 61.2 \Omega$  the admittance in the original curve is 0.0089 S. A VSWR of 2:1 represents an admittance in the original curve of 0.005 S. The two edge frequencies,  $f_{low}$  and  $f_{up}$ , can be found where the phase-transformed admittance ( $Y_{Load}$ ) is one of the above. The design of the LC-section should be done so that the imaginary admittance will be cancelled at these frequencies for close to optimal impedance enhancement (for this technique). This technique works since the LC-circuit cancels the imaginary component at the three frequencies where the transformation is anticipated for, and thus real admittance (or impedance) transformation is effectively obtained.

In order to illustrate the design procedure in full, the patch antenna example shown in Figure 3.7 with the subsequent impedance data presented in Figures 3.8 and 3.9, is

matched for close to optimal impedance bandwidth with a single LC-section. The patch antenna will be matched for two conditions, VSWR of 1.5:1 and also VSWR of 2:1. The first step in the design is to find the phase-transforming transmission line length that will result in the required admittance response. A graphical approach is taken by using the Smith chart and judging when the curve exhibits symmetry around the real axis as shown in Figure 3.13. This step is identical for both bandwidth requirements, so there is no need to repeat it. The line length to accomplish this for the patch antenna considered is  $37^\circ$  at the centre frequency, 1.8 GHz.

The first design is for optimum VSWR 2:1 bandwidth. The admittance edges for this VSWR are between 0.01 S and 0.04 S. The original real admittance is 0.02 S, so a transformer is needed to transform 0.02 S to 0.01 S using (13).

$$\begin{aligned} Z_{\lambda/4} &= \frac{1}{\sqrt{0.01 \cdot 0.02}} \\ &= 70.7\Omega \end{aligned}$$

To obtain the maximum admittance that will be transformed to acceptable admittance edges, (14) is implemented with the now known impedance  $Z_{\lambda/4}$ .

$$\begin{aligned} Y_L &= \frac{1}{0.04 \cdot 70.7^2} \\ &= 0.005S \end{aligned}$$

The frequencies where the admittance is 0.005 S (Refer to Figure 3.15) are at 1.702 GHz and 1.916 GHz. These are the frequencies where the LC-circuit must cancel the imaginary component of the admittance. The imaginary admittances at these frequencies are 0.0067 and  $-0.0066$  S respectively (Refer to Figure 3.14). The frequency with its imaginary admittance is taken and substituted into (8) and (9) for the different frequencies considered. This leaves one with two unknowns ( $L$  and  $C$ ) and two equations (an equation for the lower and upper frequency). A capacitance of 4.936 pF and inductance of 1.572 nH result in the

required LC-combination. The proposed feed network for the antenna is shown in Figure 3.20.

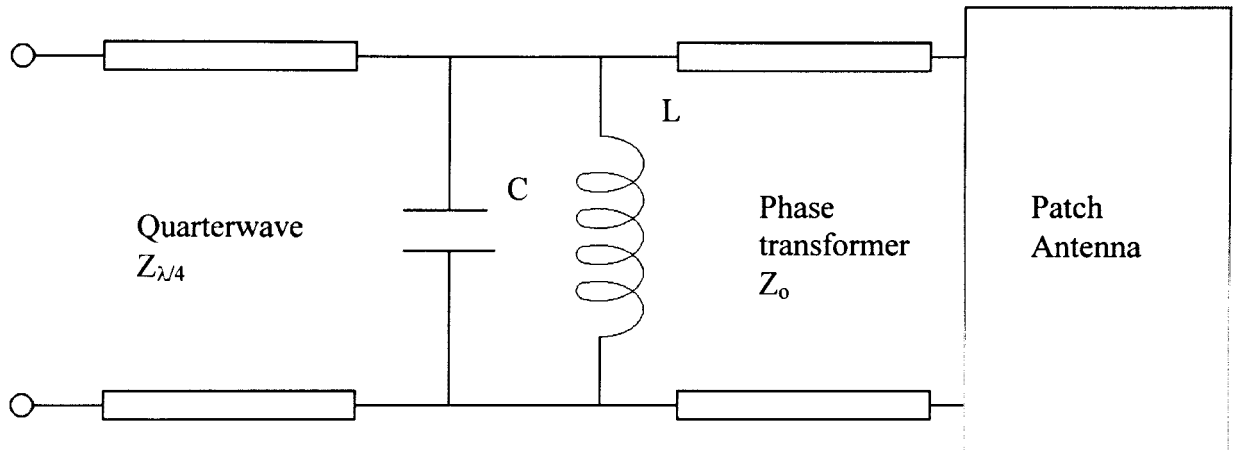


**Figure 3.20 Final feed network layout for the enhancement of microstrip patch antennas**

A summary of the resulting values for the circuit shown above with the patch antenna example of this chapter is given in Table 3.1. The quarterwave transformer value was changed from  $70.7 \Omega$  to a slightly lower value of  $70.4 \Omega$  for the VSWR of 2:1 design. The Smith chart graphical presentation is shown in Figure 3.21.

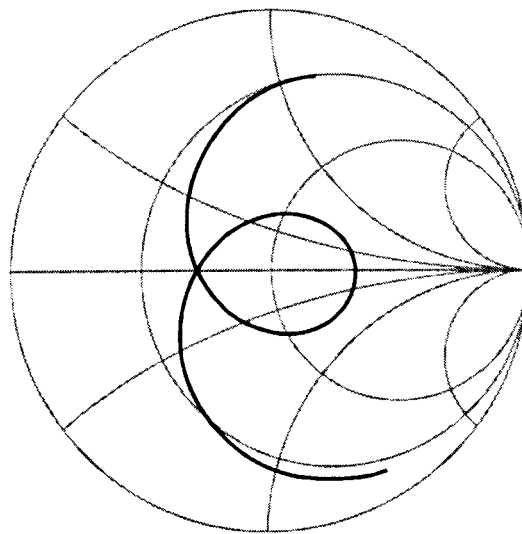


**Figure 3.21 Graphical presentation of the matching result for a VSWR < 2:1**

The return loss of the matched antenna and the original return loss of the antenna are shown in Figure 3.22. The results presented are for ideal components. The values are exact and the transmission lines lossless. In Figure 3.22 it is evident how close the centre frequency is to the VSWR specified value. For this the transforming impedance was changed slightly from 70.7 to 70.4  $\Omega$ . It is a slight variation, and resulted in the return loss at the centre frequency being just below specification instead of slightly above.

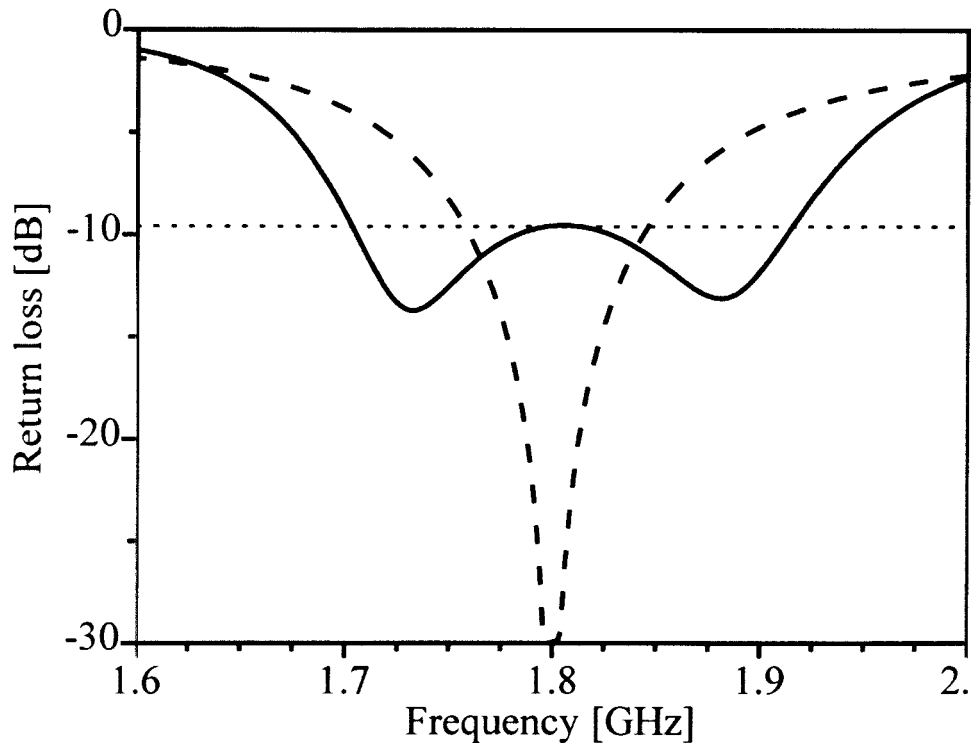


**Figure 3.22 Return loss for the matched antenna with VSWR < 2:1**

The frequency range of the antenna changed from 1.758 - 1.846 GHz to a frequency band of 1.704 - 1.914 GHz. This is an improvement from 4.89% to 11.67%, an improvement factor of 138.6%, for a VSWR of 2:1.

The same design procedure was followed for a VSWR specification of 1.5:1. The phase transformation for both scenarios remains the same. The second part of the design, to obtain a value for the capacitor and inductor, has to be repeated. From (13) the transmission line characteristic impedance for the transformer is 61.2  $\Omega$ . Substituting this impedance in (14) and using the edge's highest allowable admittance, 0.03 S, the

admittance on the real curve to be considered is 0.0089 S. The frequencies where this admittance is obtained are 1.736 and 1.87 GHz. The phase transformed imaginary admittances at these frequencies are 0.0087 and  $-0.0087$  S respectively. The calculated component values are  $C = 10.142$  pF and  $L = 0.768$  nH. The characteristic impedance for the transformer was lowered from 61.2 to 61  $\Omega$ , since the return loss is very close to the maximum allowable VSWR. The impedance curve is shown in Figure 3.23 on the Smith chart, and the return loss for direct comparison of the original and matched antenna is shown in Figure 3.24.

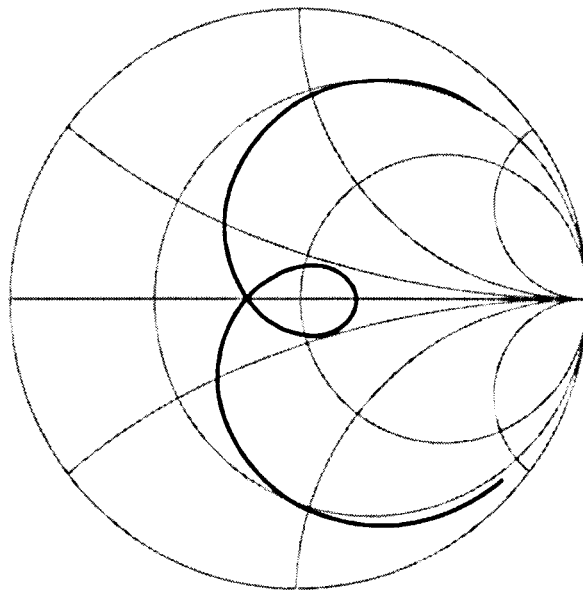


**Figure 3.23 Graphical presentation of the matched result for a VSWR < 1.5:1. The locus shown reaches the 1.5:1 VSWR circle on the right hand side of the chart, and the crossing on the left is also aimed to be right on the VSWR 1.5:1 circle.**

The frequency band of the antenna without the matching network for a VSWR of 1.5:1 is between 1.774 and 1.826 GHz. After the inclusion of the matching network with the impedance transformers a new frequency band was obtained, being 1.738-1.87 GHz. This is an improvement of 153.8%, from a bandwidth of 2.89% to 7.33%. All the results for the example presented in this section are given in Table 3.1.

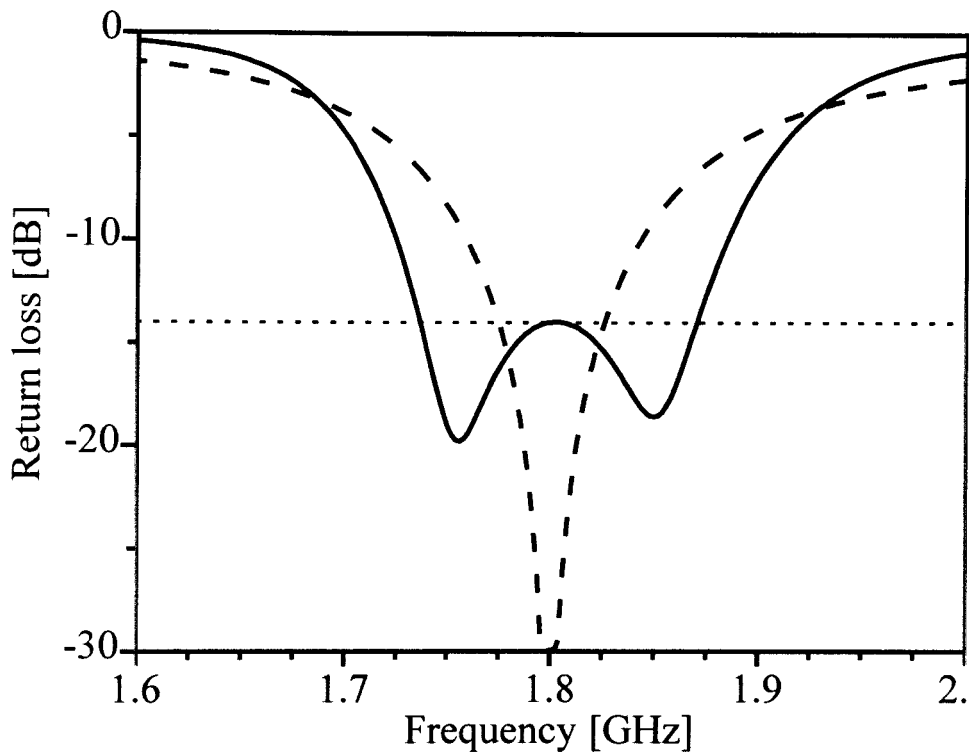


**Figure 3.24** Return loss for the matching circuit and patch antenna with VSWR < 1.5:1

**Table 3.1** Results for the matching circuit applied on the patch antenna shown in Figure 3.7

Parameter	VSWR < 2:1 Match	VSWR < 1.5:1 Match
Phase transmission line length [°]	37	37
Capacitor [pF]	4.936	10.142
Inductor [nH]	1.572	0.768
Quarterwave transformer $Z_{\lambda/4}$ [ $\Omega$ ]	70.7	61.2
Implemented $Z_{\lambda/4}$ [ $\Omega$ ]	70.4	61
Original bandwidth [MHz]	88	52
Matched bandwidth [MHz]	210	132
Improvement factor [%]	138.6	153.8

### 3.6 Conclusion on the SRMT theoretical design

From the patch antenna examples it is evident that in theory an improvement in the order of 140% can be obtained with a single LC-resonant matching circuit and some additional impedance transforming (SRMT). A comparison between the current technique (the SRMT) and results from the SRFT will be presented in the next chapter.

In chapter 4 and 5 results obtained with IE3D by Zeland Software [40] and Sonnet Lite [41] will be shown. IE3D is a full wave simulation package that implements moment method to solve microstrip circuits and antennas. Sonnet Lite is the shareware version of Sonnet. This package is specifically aimed at solving microstrip circuits. In the Lite version limitation are imposed on the circuit size one can simulate, but fortunately the SRMT presented in this dissertation is small enough so that Sonnet Lite can simulate the circuit. The theoretical designs (with ideal components) presented in this dissertation were computed with the aid of a network simulator that is part of Sonnet Lite.

Three main antenna examples, consisting of an antenna made with substrate only, the 5 mm air spaced antenna already discussed in this chapter and a 10 mm air spaced antenna are also manufactured to verify the validity of the SRMT. An antenna similar to the quarterwave coupled line structure presented in [18] is also discussed and verified against the SRMT.